

Battery Charging Current Impact on Operational Expenditure for Hybrid Telecom Systems

Soham Thakurata
Student

Department of Electrical Engineering
National Institute of Technology
st22eem3r21@student.nitw.ac.in

N V Srikanth
Professor

Department of Electrical Engineering
National Institute of Technology
Warangal, India

Shravana K Musunuri
Engineering Manager
Caterpillar Inc.
Bengaluru, India

Abstract—Remote telecom stations incorporating renewable resources such as Photovoltaic(PV) assets, along with Lithium-ion Battery Energy Storage Systems(BESS) and Diesel Generator(DG) need to evaluate the operating expenditure over time. Majority of research based on such hybrid infrastructure sites focus on the optimal sizing of PV, BESS, and DG for reliable power output. A major factor often overlooked is that though Li-ion batteries are the primary choice for BESS systems due to high power density, and longer lifetimes, they are subject to capacity degradation due to the operating conditions, resulting in a reduction in the lifetime and increase in battery replacements. This reduced capacity increases the fuel consumption for the load profile. Transportation costs and fuel losses, due to leaks and theft, also play a part in evaluation of the Operational Expenditure(OPEX). In this paper, we have sought to evaluate the impact of all these factors on the OPEX of an off-grid system.

Keywords—Photovoltaic, BESS, Operating Expenditure(OPEX), Capacity Degradation, Capacity Fade, Battery Lifecycle, State of Charge(SOC), Capacity cycling, Telecom Hybrid System

I. INTRODUCTION

Telecommunications is an indispensable part in the current world. All industries require a robust communication network, which is supplied by the telecom network. Due to its necessity, it is imperative that the data communication occurs without any interruption and should be of the highest quality. Thus, it is extremely important that the telecom towers, hosting the devices for communication, be provided with uninterrupted power supply. In parts of the world with proper grid connectivity and grid reliability, the major component of the power supply is taken from the grid itself. However, many areas still lack proper infrastructure for grid power and outages are common, with some areas too remote for effective connectivity. In these regions, the power supply is regulated by using distributed generation resources, such as Diesel generator, photovoltaic array, wind energy, battery energy storage, etc. The battery energy storage systems(BESS) are primarily based on Lithium-ion battery chemistry, due to their high efficiency, high power density, longer lifecycles and reduced cooling requirement. Lower recharge times also contribute to their growing applications in a significant manner.

Apart from the control aspect of hybrid telecom microgrid, the economic viability is an important aspect to be considered. Due to the variability of the renewable and high cost of diesel fuel, a lot of research is focused on discussing the optimal sizing of components in the case of off-grid systems to ensure reliability and minimising the capital costs. Ref [1] analyses a method in which the optimal capacity, based primary of economic cost, of PV, Wind Turbine, BESS and DG is

considered, with a case study quantified for the different combinations of the renewable resources. The paper calculates the Net Present Cost and Cost of Energy for different combinations, concluding the best solution being a combination of PV, BESS and DG. Ref [2] discusses an application of telecom industry where an Algerian Base Trans-receiver station (BTS) site to evaluate the viability of the site. However, the impact of BESS was not clarified. Ref [3] [4] illustrate the sizing and design procedure for a microgrid with PV, WT, DG and BESS units using various economic indices for the units themselves. While the processes adopted in this domain stem from the availability of the renewable resources, a simplified battery model is generally utilised, in which the capacity is maintained to be constant throughout its lifetime.

Lithium batteries utilise electrochemical reaction to deliver power from the stored chemicals in the cells. With various chemical materials available, it is imperative for the system owners to choose the most effective type of battery, depending on the system requirements. Li-ion Ferrous Phosphate(LFP) and Li-Nickel Manganese Cobalt(Li-NMC) are two of the most used commercially available types. However, Li-NMC is generally favored due to its higher specific capacity. Owing to the chemical reactions at anode and cathode, the capacity of the batteries degrade over time, both during operation and idle state [5]. Factors impacting the deterioration of the capacity can stem from temperature, battery design, current cycling rate, etc. Ref [6] discusses the capacity degradation mechanism regarding the transition metals in the electrodes with suppression mechanism. Ref [7] discusses the side reactions' effect on the battery cells' electrodes that give rise to capacity fade during cycling.

Cycling is the process during operation where the State of Charge(SOC) is repeatedly cycled through from a higher state to a lower state and vice-versa. From an operator's perspective, the discharge rate is primarily designed to supply the load, making the controllable factor to be the charging current rate. Thus, for the purposes of this paper, the cycling current is considered to be of particular interest for its effect on the capacity fade. Ref [8], [9], [10], [11] discusses various research undertaken with Li-ion cells in laboratory conditions, which observed the inverse effect of increasing charging rates on the Li-ion batteries capacity fading. Ref [12] shows a deterioration of the battery lifetime as the charging rate is increased. Ref [13] considers three cells with different charging rates. An interesting point to note is that the charging current is kept same for the three cases. Li-NMC batteries are more prone to thermal runaway at lower temperatures than LFP battery, a condition in which the chemical reaction becomes a selfsustaining exothermic reaction, as investigated in [14]. As the research suggests, all the laboratory tests conducted were based on batteries of very small capacity,

possibly due to economic and safety considerations. The results obtained above, were extrapolated with additional inputs for the purposes of this paper

In this paper, the OPEX is calculated taking into account the fuel consumption and any losses parallel to real scenarios and the effect of capacity degradation of the BESS influencing the charging and discharging times. The considered system consists of one DG, one PV array and one BESS unit of suitable capacity. In section II, a mathematical model is developed for the system components and the objective function is defined. Section III discusses the results obtained thereof and also illustrated some additional points that factored into this work.

II. MATHEMATICAL MODEL

A. System Specification

An isolated off-grid DC Telecom system of 48V DC bus is used with the following assets:

- Diesel Genset
- Photovoltaic Array
- Battery Energy Storage System
- Constant 2 kW Load

The DG set, rated for 400V, 13.5 kVA, is connected to a PEC(power electronic converter) module consisting of a rectifier(AC/DC conversion) and a step-down converter module for providing power at the rated DC bus. The PV array is rated at a 3.5 kW power @ 1 kW/m² irradiance. A Li-ion NMC battery is used as a energy storage solution, rated at 52V, with a rated capacity of 300 Ah. A constant load of 2 kW is assumed, due to small fluctuation of load in telecom towers, for which the system is designed for. The system diagram is shown in Fig 1.

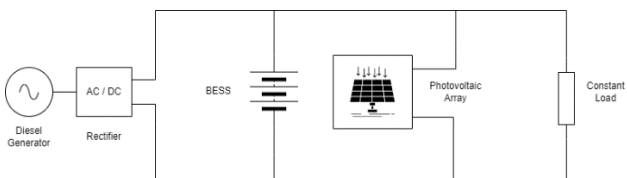


Fig 1: System Diagram

The operating expenditure(OPEX) of a system is defined as the cost incurred during the operation over a period of time under consideration. The objective of this paper is to calculate and evaluate the effects of the factors outlined on the OPEX of the system over a period of 10 years.

B. Battery Energy Storage System(BESS)

During battery cycling, one cycle is considered to be when the SOC drops from 90% to 10% and back. The expenditure with regards to the BESS are as follows:

1) Capacity Degradation:

As the number of cycle progresses, the capacity of the battery to provide energy decreases, which is evident by the effective reduction of the capacity measured by methods which are illustrated in [15]. This effect is termed as Capacity

Degradation. Due to a lack of standard capacity degradation data based on the influence of charging and discharging current, a life cycle is assumed, with the equation of the form:

$$C_{eff} = a(x) \cdot n + b(x) \quad (1)$$

where x = Discharging current, n = cycle number, and $(a, b) \rightarrow$ coefficients of equation obtained by curve fitting

2) Charging and Discharging Time:

The discharging time is defined by the time taken by the battery to reach a SOC value of 10 % from a value of 90%, and is given by

$$T_{dis} = (0.8) \cdot \frac{C_{eff}}{x_{load}} \quad (2)$$

Where, $x_{load} = \frac{P_{load}}{V_{DCBus}}$, The term 0.8 appears since the capacity cycled through is 80% of the total capacity. When the battery is charging, the time associated with the rise in SOC from 10% to 90% is termed as charging time, given by,

$$T_{ch} = (0.8) \cdot \frac{C_{eff}}{x} \quad (3)$$

where x = controlled charging current.

So,

$$T = T_{dis} + T_{ch} \quad (4)$$

where, T = Total time for one complete cycle.

Based on the charging current used, the maximum cycles that is available from the battery unit is calculated as,

$$N_{maxcycles} = l \cdot x^3 + m \cdot x^2 + n \cdot x + o \quad (5)$$

where the coefficients are selected based on 3rd order polynomial extrapolation.

C. Diesel Generator Set

The Diesel Generator is an important component of the hybrid system, being used as a backup power supply to charge the battery and also supply the load during charging time. As such, the DG consumes fuel to produce the power necessary, as directed by the controller used. The fuel consumption, and hence, its cost, forms an important aspect of the expenditure of the system. The fuel supply of the DG is realised by the presence of a fuel tank on-site, which is refilled when the fuel level reaches a certain minimum level. In response, an order is placed for a refuelling truck to refuel the tank on the premises. Due to this procedure, there are three main components to DG cost:

- Fuel Cost
- Transportation Cost
- Servicing Cost

Fuel cost is the cost of refuelling the on-site tank, transportation cost is the fixed cost associated with placing the order for the refuelling. The servicing cost is associated with DG maintenance, undertaken after a set number of hours the DG has run. Generally the duration for servicing is set at around 400 to 700 hours of DG run. The fuel tank capacity is considered to be of 1000 Litres, in this example.

During transportation, a certain amount of fuel is bound to be lost, owing to the theft, leaks, etc. This is considered and modelled as a loss, where the effective cost incurred is calculated based on the fuel developed, lost fuel amount and the resulting extra transportation cost required to compensate is calculated.

Let k = loss factor(in %), FC = fuel consumption, then the number of refills, from is calculated to be:

$$Refuel Cost = Cost_{fuel} \cdot N_{refuels} \quad (6)$$

where,

$$N_{refuel} = \left\lceil \frac{1}{1-k} \cdot \frac{FC}{Capacity_{Tank}} \right\rceil \quad (7)$$

and,

$$Servicing\ Cost = Cost_{servicing} \cdot \frac{T}{500} \quad (8)$$

The fuel consumption is calculated on basis of the time for which the DG is operational and is charging the battery, while simultaneously supplying the load, given by,

$$Fuel\ Consumption = FC(x) \cdot T_{ch} \quad (9)$$

where, x = charging current.

D. Photovoltaic Array and Load

The PV array is modelled to start produce power from 7 am in the morning to 5 pm in the evening, with a increasing irradiance until 12pm, from whence, it decreases. The solar panel's maximum power producing capability is 3.5 kW in this paper. For the purposes of simplified case study, the power production profile is considered to be the same every day for the entire span of operation. In consequence of this assumption, the actual power production can be effectively reduced to a constant power of a magnitude, calculated as below,

$$P_{PV,effective} = \alpha \cdot P_{PV,maximum} \quad (10)$$

where α = constant. α value is calculated by using the fact that the total energy of the PV during a day can be approximated by using the maximum power supply, $P_{PV,maximum}$ and converting it into a constant power supply, which is $P_{PV,effective}$. From this result, the virtual load can be considered to be,

$$P_{load,effective} = P_{load} - P_{PV,effective} \quad (11)$$

E. Objective

The objective function considered is the sum of the various components consider, as explained below.

$$Minimise OPEX = OPEX_{DG} + OPEX_{Battery} \quad (12)$$

where,

$$OPEX_{DG} = Cost_{fuel} + Cost_{transportation} + Cost_{servicing}$$

$$OPEX_{Battery} = RC \cdot (Number\ of\ Replacements) \quad (13)$$

where RC = Replacement Cost for Battery. Number of replacements for the battery is calculated by using the algorithm outlined in section II-F.

F. Algorithm for Cost Calculations

The algorithm used to calculate the expenditures due to various components is illustrated in this section. It is developed by considering an entire charge-discharge cycle as a single unit for iteration, thus, the dynamics of the system is ignored and the costs are calculated on the energy exchanged during the lifetime of the project

```

1: T = T_dis = Tch = 0 and N_battery = 0
2: while T ≤ Total Hours do
3:   for n = 1 to N do
4:     Calculate T_dis and T_ch from (2) and (3)
5:   if T ≥ TotalHours then
6:     exit
7:   end if
8:   end for
9: N_battery + 1
10: end while
11: Calculate fuel consumption, refills and OPEX values
    from (9) (6) (12) and (13)
  
```

The value of $N_{battery}$ provides the value of the replacements required for equation (13).

III. RESULTS AND DISCUSSION

A. OPEX Calculation using Different Lifecycle Profile

The minimum of the operational expenditure of the systems is calculated using MATLAB. There are two lifecycles used for comparison in this study. They are illustrated in Fig2 and Fig 3.

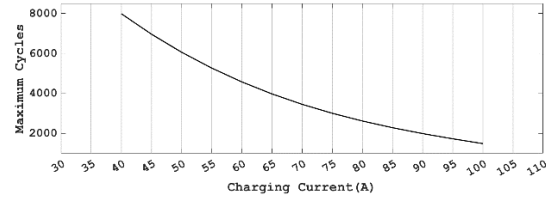


Fig 2. Battery Lifecycle 1

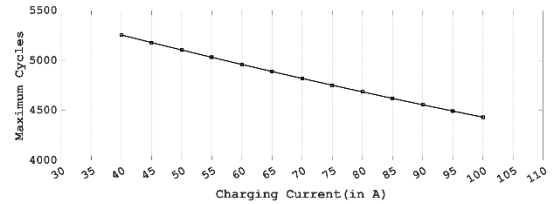


Fig 2. Battery Lifecycle 2

Pursuant to these two lifetime cycles available for the Li Batteries considered, the operating expenditure for these are evaluated, with component cost breakup. The Figures shown in Fig 4 and Fig 5 corresponding to the two different cycles considered before, without any photovoltaic power production. The various costs considered for the above calculations are:

- Diesel Fuel cost = \$ 1.4 per Litre
- Battery Cost = \$ 4000;
- Servicing cost = \$ 100 per servicing;
- Transportation Cost = \$ 1000 per trip

From 4, it can be observed that, as the charging current is increased, the fuel consumption decreases. The battery cost, however, behaves contrary to the fuel curve. This can be attributed to the fact that as the charging current increases, the lifetime of the battery is affected inversely, owing to the rate of chemical reactions and physical stresses associated with higher charging rates affecting the battery electrodes. Thus, to meet the load requirement of the system, more number of batteries are required. The minimum cost of operation, due to the conflicting natures of the two factors, occurs at a charging current values of 65 A, 75 A and 80 A. Hence, for this system, it can be recommended that the appropriate charging current should about 80 A for minimising the OPEX for 10 years.

From Fig 5, the profile shows an expected decreasing curve with rising charging current. The battery cost, in this case, however, shows a single change in value. The reason for this can be attributed to the fact that the lifetime of the battery is not affected in a significant manner when using it at 100 A changing current, as compared to 40 A charging current,

evident from Fig3. Due to this the decreasing curve of the fuel overpowers the battery cost change, resulting in the minimum expenditure values to be for values of current on the higher specified limits' end. In this system, the recommended charging current can be in 90 A to 100 A range for minimum OPEX during 10 years of operation.

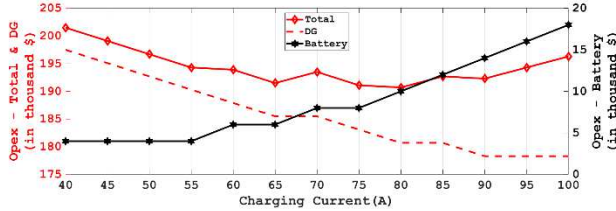


Fig. 4. OPEX breakup for 1st Cycle

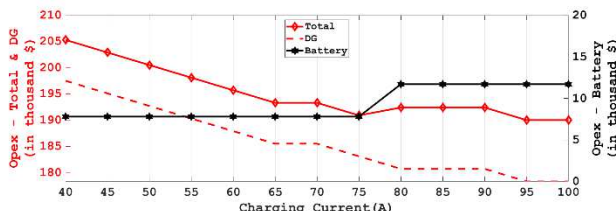


Fig. 5. OPEX Breakup for 2nd Cycle

Considering solar power output into the cost calculation, Fig 6 and Fig. 7 are obtained. With respect to the results, the calculation methodology adopted in II-D, the load power effectively reduces. It is interesting to note that the minimum cost for the 1 st cycle shifts slightly towards 85 A. With respect to 2 nd cycle in Fig 7, the number of battery replacement is remains to be one.

The total OPEX is plotted for a variation of cost for BESS for replacement, in Figures 8 and 9. Note that the reduction with regards to the 2 nd cycle is significantly more than that of the 1 st. It can also be observed that, in Fig 8, the cost increases past the minimum charging current of 80 A, due the increasing nature of battery costs overtaking the reduction in the fuel consumption costs. It can be noticed that the difference between successive OPEX increases as the charging current increases. This can be directly attributed to the number of replacements times the difference between the battery costs.

The impact of fuel transportation costs and fuel cost was also calculated, based on the lifecycle shown in Fig 2, as shown in Fig 10 and Fig 11. From the above figures, it can be observed that as the transportation and fuel costs decrease, the OPEX is directly affected. Based on the load profile of the system's application, the cost associated with the fuel in OPEX will increase as the fuel cost increases. Contribution of transportation costs is dependent on the fuel loss during transportation and fuel consumption. As the transportation losses are unavoidable, owing to the region of the telecom site and the supply routes available, as the fuel prices increase, the designer should prioritise suppliers offering lower fuel transportation costs.

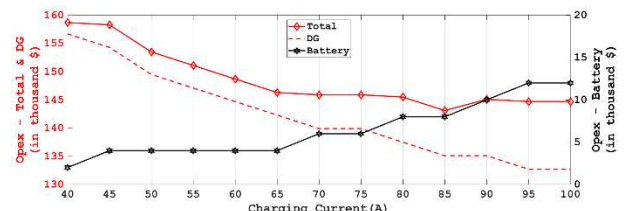


Fig. 6. OPEX for 1st Cycle (with PV)

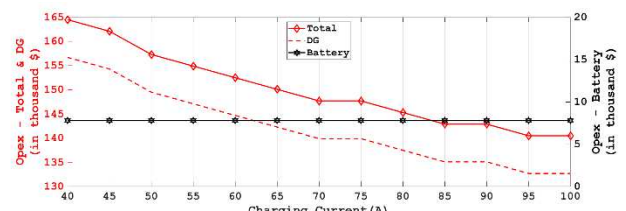


Fig. 7. OPEX for 2nd Cycle (with PV)

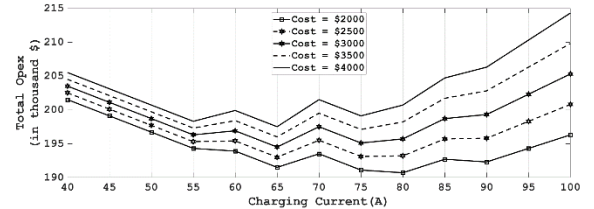


Fig. 8. OPEX Variation for 1st

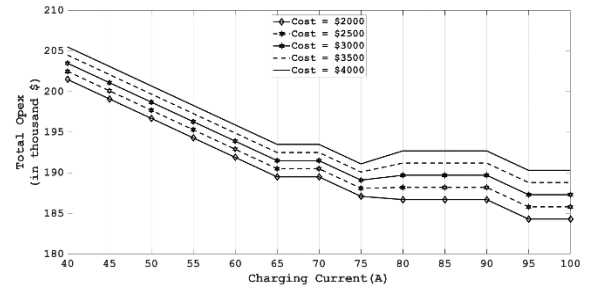


Fig. 9. OPEX Variation for 2nd

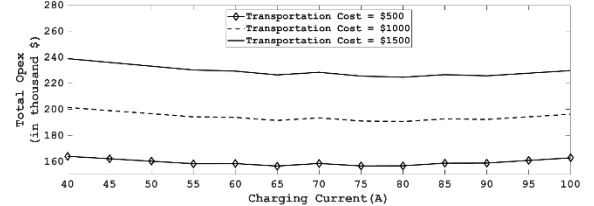


Fig. 10. Total OPEX Variation on Transportation Cost - 1st cycle

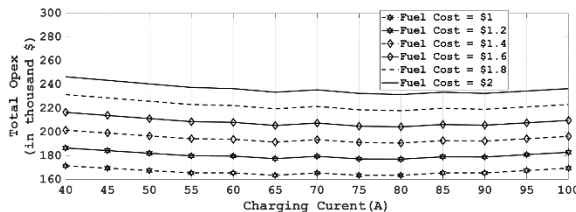


Fig. 11. Total OPEX Variation on Fuel Cost - 1 st cycle

B. Additional Comments

Based on literature review, an important point needs to be highlighted. The method for calculating or reading lifetime for current cycling in battery systems is undertaken by cycling a constant current during charging and discharging cycles. It is not clear, therefore, if the lifetime of battery is affected in a manner similar to this method of the charging and discharging currents are of different values during one complete cycle. In this work, it is assumed the lifetime effect is similar in both cases.

The battery is considered for replacement when the BESS capacity drops to or below 70% of its initial capacity, which occurs due to chemical reaction and degradation of electrodes and the electrolyte. The capacity degradation during cycling is considered on a per cycle basis, i.e. the capacity curve values are provided for the measured capacity at the end of each cycle. Here it is assumed that the time taken by the battery to charge or discharge is virtually unaffected by the changing capacity during a single charging cycle consisting of one discharge and one charge.

IV. CONCLUSION

It was observed that the OPEX depends on a variety of factors, which have been considered in this paper. A mathematical framework was utilised to study the operational cost of a hybrid energy system over the considered lifetime. Real-world scenarios involve the effect of battery degradation, battery cost, transportation cost and fuel cost on the OPEX, which have been considered in this paper for a period of ten years. The fuel and transportation costs(losses included) depend on the location of site. The discharge current of the BESS is dependent on the load and PV output but the selection of BESS charging current can be made based on lifecycle degradation data to optimise the OPEX. Two discharge current based lifecycles degradation curves of batteries was used to compare the OPEX evaluation along different charging currents. A strong relationship was observed between the lifecycle degradation and OPEX variation, resulting in corresponding selection of charging current. The impact of fuel cost, transportation costs and battery costs on the OPEX of the entire system was also calculated. The designer of a hybrid energy system for telecom application needs to consider the factors outlined above, in order to minimise the OPEX of the system. This paper provides an insight how the selection of charging current is affected by battery degradation, in addition to other exogenous factors such as fuel and transportation costs.

ACKNOWLEDGMENT

I would like to thank Caterpillar Inc. for the providing this opportunity for research. I would also like to thank my guide

Dr N V Srikanth for guiding me throughout this whole project and Shravana K Musunuri for his invaluable inputs and his expertise on this research

REFERENCES

- [1] V. V. V. S. N. Murty and A. Kumar, "Optimal energy management and techno-economic analysis in microgrid with hybrid renewable energy sources," *Journal of Modern Power Systems and Clean Energy*, vol. 8, no. 5, pp. 929–940, 2020
- [2] M. A. Z. M. L. A. Z. S. K. M. and Z. S. A., "Simulation and optimization of hybrid system (photovoltaic panel and diesel generator with energy storage) for base transceiver (bts) station site located in southern algeria," in 2023 Second International Conference on Energy Transition and Security (ICETS), 2023, pp. 1–7
- [3] L. J. Olatomiwa, S. Mekhilef, and A. S. N. Huda, "Optimal sizing of hybrid energy system for a remote telecom tower: A case study in nigeria," in 2014 IEEE Conference on Energy Conversion (CENCON), 2014, pp. 243–247
- [4] F. Nejabatkhah, Y. W. Li, A. B. Nassif, and T. Kang, "Optimal design and operation of a remote hybrid microgrid," *CPSS Transactions on Power Electronics and Applications*, vol. 3, no. 1, pp. 3–13, 2018
- [5] W. Vermeer, G. R. Chandra Mouli, and P. Bauer, "A comprehensive review on the characteristics and modeling of lithium-ion battery aging," *IEEE Transactions on Transportation Electrification*, vol. 8, no. 2, pp. 2205–2232, 2022
- [6] C. Zhan, T. Wu, J. Lu, and K. Amine, "Dissolution, migration, and deposition of transition metal ions in li-ion batteries exemplified by mn-based cathodes – a critical review," *Energy Environ. Sci.*, vol. 11, pp. 243–257, 2018. [Online]. Available: <http://dx.doi.org/10.1039/C7EE03122J>
- [7] R. Xiong, Y. Pan, W. Shen, H. Li, and F. Sun, "Lithium-ion battery aging mechanisms and diagnosis method for automotive applications: Recent advances and perspectives," *Renewable and Sustainable Energy Reviews*, vol. 131, p. 110048, 2020. [Online]. Available: <https://www.sciencedirect.com/science/article/pii/S1364032120303397>
- [8] G. Sarre, P. Blanchard, and M. Broussely, "Aging of lithium-ion batteries," *Journal of Power Sources*, vol. 127, no. 1, pp. 65–71, 2004, eighth Ulmer Electrochemische Tage. [Online]. Available: <https://www.sciencedirect.com/science/article/pii/S0378775303009388>
- [9] G. Ning, B. Haran, and B. N. Popov, "Capacity fade study of lithium-ion batteries cycled at high discharge rates," *Journal of Power Sources*, vol. 117, no. 1, pp. 160–169, 2003. [Online]. Available: <https://www.sciencedirect.com/science/article/pii/S0378775303000296>
- [10] T. Guan, S. Sun, F. Yu, Y. Gao, P. Fan, P. Zuo, C. Du, and G. Yin, "The degradation of licoo₂/graphite batteries at different rates," *Electrochimica Acta*, vol. 279, pp. 204–212, 2018. [Online]. Available: <https://www.sciencedirect.com/science/article/pii/S0013468618309800>
- [11] T. Guan, P. Zuo, S. Sun, C. Du, L. Zhang, Y. Cui, L. Yang, Y. Gao, G. Yin, and F. Wang, "Degradation mechanism of licoo₂/mesocarbon microbeads battery based on accelerated aging tests," *Journal of Power Sources*, vol. 268, pp. 816–823, 2014. [Online]. Available: <https://www.sciencedirect.com/science/article/pii/S037877531400977X>
- [12] L. Somerville, J. Barenco, S. Trask, P. Jennings, A. McGordon, C. Lyness, and I. Bloom, "The effect of charging rate on the graphite electrode of commercial lithium-ion cells: A post-mortem study," *Journal of Power Sources*, vol. 335, pp. 189–196, 2016. [Online]. Available: <https://www.sciencedirect.com/science/article/pii/S0378775313842>
- [13] D. Wong, B. Shrestha, D. A. Wetz, and J. M. Heinzel, "Impact of high rate discharge on the aging of lithium nickel cobalt aluminum oxide batteries," *Journal of Power Sources*, vol. 280, pp. 363–372, 2015. [Online]. Available: <https://www.sciencedirect.com/science/article/pii/S0378775315001263>
- [14] H. Shen, H. Wang, M. Li, C. Li, Y. Zhang, Y. Li, X. Yang, X. Feng, and M. Ouyang, "Thermal runaway characteristics and gas composition analysis of lithium-ion batteries with different lfp and ncm cathode materials under inert atmosphere," *Electronics*, vol. 12, no. 7,

2023. [Online]. Available: <https://www.mdpi.com/2079-9292/12/7/1603>

[15] X. Han, M. Ouyang, L. Lu, J. Li, Y. Zheng, and Z. Li, “A comparative study of commercial lithium ion battery cycle life in electrical vehicle: Aging mechanism identification,” *Journal of Power Sources*, vol. 251, pp. 38–54, 2014. [Online]. Available: <https://www.sciencedirect.com/science/article/pii/S0378775313018>